December 2006

Structural study of Mn-doped ZnO fi lms by TEM

Xingzhong Li
University of Nebraska - Lincoln, xli2@unl.edu

Jun Zhang
University of Nebraska - Lincoln, jzhang5@unl.edu

David J. Sellmyer
University of Nebraska-Lincoln, dsellmyer@unl.edu

Published in *Solid State Communications* 141 (2007), pp. 398–401.
http://www.sciencedirect.com/science/journal/00381098

Structural study of Mn-doped ZnO films by TEM

X. Z. Li *[,a], Jun Zhang [a,b], D. J. Sellmyer [a,b]

[a] *Nebraska Center for Materials and Nanoscience, University of Nebraska, Lincoln, NE 68588, USA*
[b] *Department of Physics and Astronomy, University of Nebraska, Lincoln, NE 68588, USA*

*Corresponding author — *Email*: xli2@unl.edu (X. Z. Li)

Submitted November 2006; accepted November 18, 2006 by A.H. MacDonald; published online December 6, 2006

Abstract: The structural study of diluted magnetic semiconductors is important for interpreting the ferromagnetic behavior associated with the materials. In the present work, a series of low concentration Mn-doped ZnO thin films synthesized by pulsed laser deposition was studied by electron microscopy. All films show the wurtzite structure with (001) preferred growth orientation on the Si substrate. Electron diffraction experiments indicate the deterioration of the growth orientation in some areas of the films with increasing Mn concentration, and the existence of a secondary phase, of Mn_2O_3-type, in the films with larger Mn concentrations. High-resolution electron microscopy images confirm the existence of the secondary phase in the grain boundary of the Mn-doped ZnO phase. The magnetic properties of Mn-doped ZnO are discussed in relation to the structures of the films.

Keywords: Magnetically ordered materials, Thin films, Crystal structure, Transmission electron microscopy

1. Introduction

Spintronic technologies seek to extend the properties and applications of established electronic devices by making use of the spins of electrons in addition to their charge. Compared with conventional semiconductor devices, the potential advantages of spintronic devices are to increase data processing speeds, decrease electric power consumption, and increase integration densities. Spintronic devices are dependent on the development of ferromagnetic ordering in diluted magnetic semiconductors (DMS), which are non-magnetic semiconductors doped with magnetic atoms/ions. The key need for achieving practical applications of these devices is to increase the Curie temperature T_c of DMS materials to above room temperature.

Much of the recent effort has focused on conventional II–VI and III–V semiconductor materials. For example, the highest Curie temperature T_c in Mn-doped GaAs is about 172K [1]. It has been theoretically predicted that, when suitably doped with transition metal ions (V, Mn, Fe, Co or Ni), ZnO might be made ferromagnetic with a Curie temperature higher than room temperature[2,3]. Extensive experiments have been carried out in many research groups in response to this prediction[4–9]. However, controversy between research groups was reported on the magnetic behavior of the materials. Both the absence of ferromagnetic ordering and its existence, with differing T_c values, have been reported.

In the Mn-doped ZnO system, Fukumura et al. [4] found a spin-glass behavior, Jung et al. [5] observed ferromagnetic ordering with a $T_c \sim 45$ K, and Tiwari et al. [6] did not find any ferromagnetism. Sharma et al. [7] reported a confirmation of the theoretical predication of ferromagnetism in Mn-doped ZnO; weak ferromagnetic ordering above 300K was observed in both bulk pellets and in transparent films 2–3 μm thick. The important points in the synthesis of Mn-doped ZnO DMS were noticed, i.e., (a) low concentration of Mn, and (b) relatively low-temperature treatment. However, similar experiments were carried out in other research groups, and the ferromagnetic behavior found was related to either an oxygen-vacancy-stabilized metastable phases Zn-incorporated Mn_2O_3 [8] or Zn-incorporated MnO_2 [9].

Table 1
A series of Mn-doped ZnO films studied in the present work

Nominal composition (Mn at.%)	EDS result (Mn at.%)
$x = 1$	0.78–0.92
$x = 3$	1.63–1.93
$x = 5$	2.21–2.78

Nominal concentration of Mn ($Zn_{1-x}Mn_xO$) and the results in X-ray energy dispersive spectroscopy (EDS).

Low temperature processing has the potential problem that the interactions between the MnO_2 and ZnO particles only act near the interfaces, as shown by the fact that the actual concentration of Mn in ZnO is much less than the nominal value. This will create a difficulty for the Mn-doped ZnO DMS in bulk or powder form. This problem can be avoided for Mn-doped ZnO film by pulsed laser deposition (PLD), since a low-temperature process such as PLD is effective for making more magnetic ions soluble in the ZnO than in the bulk under equilibrium conditions[10].

A series of Mn-doped ZnO films were synthesized by the PLD method, and ferromagnetic ordering was detected in these low concentration Mn-doped films [11]. In the present work, we report the results of a systematic electron microscopy/diffraction study of the crystalline growth of and any secondary phases in the thin films, which are the two crucial points in the interpretation of the magnetic properties of the transition-metal-doped DMS thin films.

2. Experiment

Mn-doped ZnO ($Zn_{1-x}Mn_xO$, $x = 0.01, 0.03, 0.05$; $x = 0$ for comparison) thin films were grown on Si (100) substrates by the PLD method. The base pressure of the PLD chamber was 2×10^{-7} Torr. During film growth, the oxygen pressure in the chamber was kept at 5×10^{-4} Torr, and the substrate temperature was 500 °C. The magnetic measurements were made in a superconducting quantum interference device (SQUID) magnetometer (Quantum Design, MPMS-XL). Electron diffraction (ED) and high-resolution electron microscopy (HREM) studies were undertaken using a Jeol JEM2010 200 kV TEM equipped with X-ray energy dispersive spectroscopy(EDS). Polycrystalline electron diffraction patterns were analyzed using JECP/PCED [12], a computer program for the simulation of polycrystalline electron diffraction.

3. Results and discussion

Mn-doped ZnO ($Zn_{1-x}Mn_xO$, $x = 0.01, 0.03, 0.05$) thin films were examined by EDS, and Table 1 lists the experimental results together with the nominal Mn compositions. It is noted that the Mn concentration of the films increases with the designed concentration in the experiments; however, the concentration is less than the nominal composition for the samples with $x = 0.03$ and 0.05, and is quite close for the sample with $x = 0.01$. In the following, all films are labeled by their nominal composition for convenience.

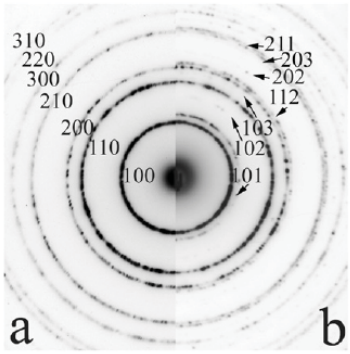

Fig. 1. Electron diffraction patterns of samples $Zn_{1-x}Mn_xO$ (a) $x = 0.01$ and (b) $x = 0.03$. The patterns are indexed using the wurtzite structure of ZnO. A deteriorated (001) preferred orientation can be noticed with additional rings in (b) in comparison with the pattern in (a).

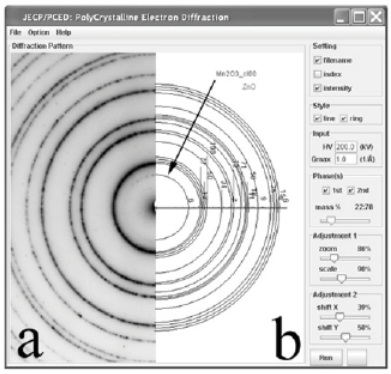

Fig. 2. (a) Electron diffraction pattern of sample $Zn_{1-x}Mn_xO$, $x = 0.05$ and (b) a simulated electron diffraction pattern of Mn_2O_3 together with ZnO. The nearest ring in Fig. 2 corresponds to the (211) reflection of Mn_2O_3.

3.1. Electron diffraction results

The electron diffraction results show that all samples $Zn_{1-x}Mn_xO$, $x = 0, 0.01, 0.03, 0.05$ on Si substrates have the wurtzite structure with a (001) preferred orientation. There is no difference in the electron diffraction patterns for $Zn_{1-x}Mn_xO$, $x = 0$ and 0.01, which is shown in Fig. 1(a). In some areas of the samples $Zn_{1-x}Mn_xO$, $x = 0.03$ and 0.05, additional rings appear in the electron diffraction pattern, which are shown in Fig. 1(b) for comparison. However, all the rings can be indexed with the wurtzite structure, which means that the (001) texture deteriorates with increasing Mn doping.

In the electron diffraction patterns taken in some areas of the $x = 0.05$ sample, additional rings are observed as shown in Fig. 2(a), which cannot be indexed with the wurtzite structure, thus indicating the existence of a secondary phase. Potential secondary phases include the manganese oxides: MnO_2, MnO, Mn_3O_4, Mn_2O_3. All Mn oxides are antiferromagnetic except Mn_3O_4, which is ferrimagnetic with $T_c = 43$ K. However, Zn-incorporated MnO_2 and Mn_2O_3 were reported to be the possible source of ferromagnetism in Mn-doped ZnO in experiments on bulk samples [8, 9].

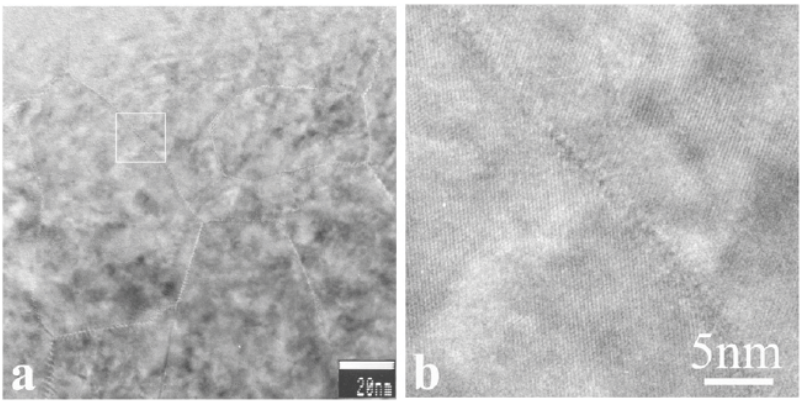

Fig. 3. (a) Plan-view HREM image of sample $Zn_{1-x}Mn_xO$, $x = 0.01$ and (b) enlarged view of a selected area in (a). The hexagonal arrangement of dots or lattice fringes can be viewed in most areas of the grain, and extends to the grain boundaries.

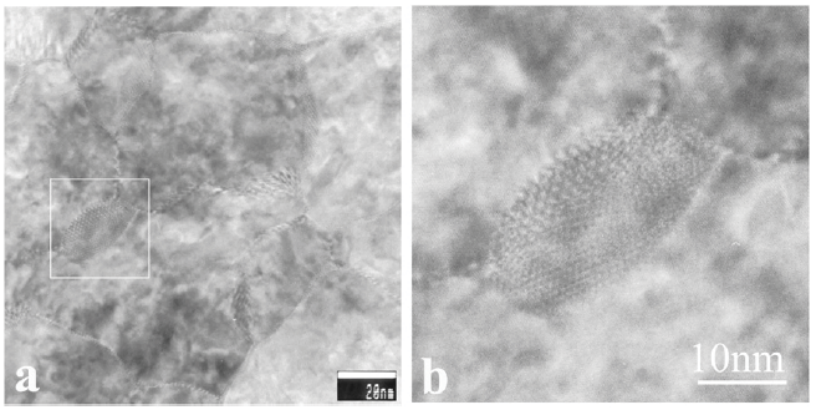

Fig. 4. (a) Plan-view HREM image of sample $Zn_{1-x}Mn_xO$, $x = 0.05$ and (b) enlarged view of a selected area in (a). A secondary phase can be identified in the boundaries of the Mn-doped ZnO phase.

Electron diffraction patterns of all manganese oxides together with ZnO were simulated using the JECP/PCED computer program for identifying the secondary phase. It was found that the extra ring in Fig. 2(a) can only be matched to the electron diffraction pattern of Mn_2O_3, which means the secondary phase has a Mn_2O_3-type structure. Fig. 2 shows (a) the electron diffraction pattern taken from sample $Zn_{1-x}Mn_xO$, $x = 0.05$ and (b) the simulated pattern of Mn_2O_3 together with ZnO phase. The simulating diffraction pattern of ZnO includes the rings of all reflections, but only the reflections of the [001] zone should be matching to the experimental ones. The nearest ring in Fig. 2 corresponds to the (211) reflection of Mn_2O_3, and the other rings from Mn_2O_3, are shadowed by the rings from ZnO, thus are not labeled here.

3.2. HREM results

Plan-view TEM samples were prepared for the structural characterization of the Mn-doped ZnO films. The HREM images taken with the film normal along the incident beam in Fig. 3 show the growth morphology of the sample with $x = 0.01$. The hexagonal arrangement of dots or lattice fringes can be viewed in the most areas of the grain, and extends to the grain boundaries. The averaged grain size is about 100 nm. The HREM images of the $x = 0$ and 0.03 samples are similar to Fig. 3.

Fig. 4 shows the HREM image of the $x = 0.05$ sample, which was taken under the same conditions as Fig. 3. The scattered distribution of the secondary phase with size less than 20 nm can be identified in the boundaries of ZnO phase, which confirms the observations from the electron diffraction experiment of the $x = 0.05$ sample.

It was reported that a secondary phase exists in the interface of TiO and its substrate for Co-doped TiO [13]. A cross-sectional TEM sample was prepared for the $x = 0.03$ sample for such an investigation. Fig. 5 shows a HREM image of the $x = 0.03$ sample, taken with the film normal perpendicular to the incident beam. It shows the smooth growth of ZnO grains in a columnar shape on the Si substrate. No precipitate was found in the interface of the Mn-doped ZnO DMS and Si substrate. The thickness of the Mn-doped ZnO film is about 75 nm.

3.3. Discussion

Hysteresis loops have been observed in the same series of samples in the present study, and the moment per Mn atom was found to decrease with an increase of Mn concentration

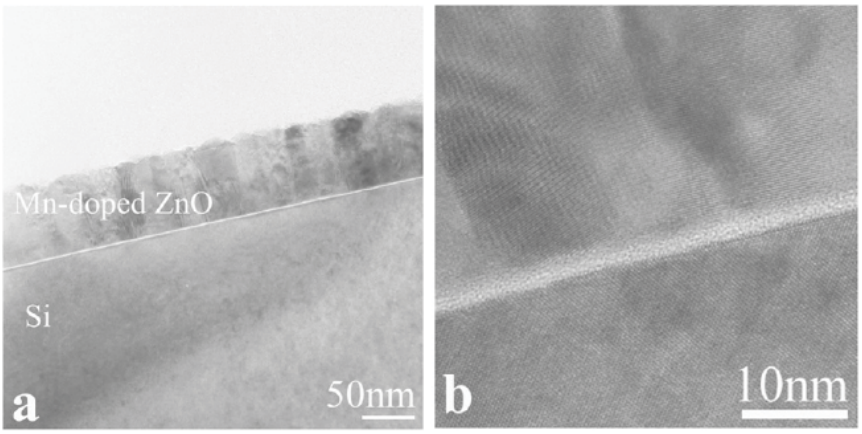

Fig. 5. (a) Cross-sectional HREM image of sample $Zn_{1-x}Mn_xO$, $x = 0.03$ and (b) enlarged view of a selected area in (a). It shows the smooth growth of ZnO grains in a columnar shape on the Si substrate. No precipitate was observed in the interface of Mn-doped ZnO DMS and Si substrate.

[11]. This shows that ferromagnetic ordering exists in the low concentration Mn-doped ZnO thin films on Si synthesized by pulsed laser deposition. The TEM study confirms that the magnetic ordering in the Mn-doped ZnO film does not originate from a Mn_2O_3-type of secondary phase, since there are no secondary phases in the samples for $x \leq 0.03$, and the magnetic moment decreases when the Mn_2O_3 type of secondary phase exists in a sample $Zn_{1-x}Mn_xO$, $x = 0.05$.

Ferromagnetic ordering was also observed by Norton et al. [14] in Mn-doped *n*-type ZnO with a T_c of ~250 K, in ZnO single crystals co-doped with Mn (3 at.%) and Sn; it was also found that the magnetic moment decreases with the increase of Mn up to 5 at.%. An inverse correlation between magnetization and electron density as controlled by Sn doping was reported [15]. It is worth pointing out that ZnO without any *p*-type doping is an intrinsic *n*-type semiconductor. The inverse correlation is in agreement with that the color of the pellets processed at low temperature, which are whitish and more like stoichiometric ZnO, but change to yellow on processing at high temperatures, suggesting an increase in *n*-type carriers[7].

4. Summary

In the present work, electron diffraction and high-resolution electron microscopy have been used for the structural characterization of Mn-doped ZnO films. The results show that a Mn_2O_3-type secondary phase exists in 5 at.% Mn-doped ZnO film. Although the mechanism of the formation of ferromagnetism in this system is unclear so far, it has been determined that the ferromagnetic ordering in the low-concentration Mn-doped ZnO films on Si substrate does not originate from a secondary phase.

Acknowledgments

We would like to thank Professor Y. F. Lu for allowing us to use the PLD equipment in the Laser Assisted Nano Engineering Laboratory (LANE), University of Nebraska. This research is supported by NSF-MRSEC, W. M. Keck Foundation, Nebraska Research Initiative (NRI) and Nebraska Center for Materials and Nanoscience (NCMN).

References

[1] A.M. Nazmul, S. Sugahara, M. Tanaka, Phys. Rev. B 67 (2003). art241308.

[2] T. Dietl, H. Ohno, F. Matsukura, J. Cibert, D. Ferrand, Science 287 (2000) 1019.

[3] K. Sato, H. Katayam-Yoshida, Jpn. J. Appl. Phys. 39 (2000) L555.

[4] T. Fukumura, Z. Jin, M. Kawasaki, T. Shono, T. Hasegawa, S. Koshihara, H. Kionuma, Appl. Phys. Lett. 78 (2001) 958.

[5] S.W. Jung, S.-J. An, G.-C. Yi, C.U. Jung, S.-I. Lee, S. Cho, Appl. Phys. Lett. 80 (2002) 4561.

[6] A. Tiwari, C. Jin, A. Kvit, D. Kumar, J. Muth, J. Narayan, Solid State Commun. 121 (2002) 371.

[7] P. Sharma, A. Gupta, K.V. Rao, F.J. Owens, R. Sharma, R. Ahuja, J.M.O. Guillen, B. Johansson, G.A. Gehring, Nat. Mater. 2 (2003) 673.

[8] D.C. Kundaliya, S.B. Ogale, S.E. Loflano, S. Dhar, C.J. Metting, S.R. Shinde, Z. Ma, B. Varughese, K.V. Ramanujachary, L. Salamanca-riba, T. Venkatesan, Nat. Mater. 3 (2004) 709.

[9] M.A. Garcia, M.L. Ruiz-Gonzalez, A. Quesada, J.L. Costa-Kraemer, J.F. Fernandez, S.J. Khatib, A. Wennberg, A.C. Caballero, M.S. Martin-Gonzalez, M.Villegas, F. Friones, J.M. Gonzalez-Calbet, A. Hernando, Phys. Rev. Lett. 94 (2005). art217206.

[10] K. Ueda, H. Tabata, T. Kawai, Appl. Phys. Lett. 79 (2001) 988.

[11] J. Zhang, X.Z. Li, L.P. Yue, J. Shi, Y.F. Lu, D.J. Sellmyer, J. Phys.: Condens. Mat. (2006) (submitted for publication).

[12] X.Z. Li, Ultramicroscopy 99 (2004) 257.

[13] S.R. Shinde, S.B. Ogale, J.S. Higgins, H. Zheng, A.J. Millis, V.N. Kulkarni, R. Ramesh, R.L. Greene, T. Venkatesan, Phys. Rev. Lett. 92 (2004). art166601.

[14] D.P. Norton, S.J. Pearton, A.F. Hebard, N. Theodoropoulou, L.A. Boatner, R.G. Wilson, Appl. Phys. Lett. 82 (2003) 239.

[15] M. Ivill, J. Pearton, D.P. Norton, J.Kelly, A.F. Hebard, J. Appl. Phys. 97 (2005). art053904.